

Cleaning of Solid Behenic Acid Residue from Stainless-Steel Surfaces

Christine S. Grant, Alan T. Perka, William D. Thomas, and Rashmi Caton
Dept. of Chemical Engineering, North Carolina State University, Raleigh, NC 27612

A rotating disk apparatus was used to study the removal of C¹⁴ labeled docosanoic (behenic) acid from stainless steel. The liquid cleaning behavior was studied as a function of temperature, surface morphology, and fluid flow. A mass-transfer model was proposed to describe the removal of behenic acid from stainless steel using a rotating disk apparatus. The cleaning rates computed from the mass-transfer model were compared with experimental observations; it was found that at low temperatures the removal was a function of rotation speed. At higher temperatures, however, the removal rate was independent of the disk rotation speed. In some cases the predicted rate of behenic acid removal differed significantly from the observed data. A plausible explanation for these variations is that the residues are removed by the combined effects of dissolution and the shearing of large clusters of solid behenic acid crystals. The temperature-dependent behavior of the cleaning data was analyzed using an activation-energy-based model.

Introduction

The cleaning of chemical processing vessels is a significant source of solvent wastes. This is particularly true for vessels used in batch processing, which often require cleaning between each batch. The research presented here is part of a study aimed at improving the understanding of mass-transfer mechanisms that control solvent-based cleaning processes. The ultimate goal of this research is to suggest ways to minimize the waste that is generated during vessel cleaning.

A literature search on vessel cleaning revealed a number of empirical studies, emanating primarily from the food processing industry (Perka, 1991; Perka et al., 1993). Cleaning studies in the literature have typically taken the approach of collecting soil removal data and then attempting to explain the results in terms of kinetic models (Jennings, 1965; Gallot-LaVallee et al., 1982; LeClercq-Perlat and Lalande, 1991), although the fundamental basis for using a kinetic model is unclear. Attempts have been made to explain results from the various cleaning studies in terms of diffusion and chemical reaction principles, most notably by Plett (1985), but a comprehensive fundamental treatment is still needed.

This article focuses on the removal of residues by the liquid phase during cleaning and the effect of the surface mor-

phology of the residue on the mass-transfer behavior. Experiments were conducted on the removal of behenic acid (docosanoic acid), a straight-chain carboxylic acid with the formula $\text{CH}_3(\text{CH}_2)_{20}\text{CO}_2\text{H}$, from stainless steel using ethanol as the solvent. Behenic acid was chosen as the residue for the experimental work for two reasons: (1) it is chemically similar to other compounds (e.g., stearic acid, tristearin) which have been used in earlier published cleaning studies (Anderson et al., 1959; Anderson et al., 1960; Harris et al., 1961; Harris and Satanek, 1961a,b), and (2) behenic acid is typically processed in stainless-steel reactors, which are then cleaned by either refluxing or filling and draining with denatured alcohol or acetone (Perka, 1991). Ethanol was selected as the solvent for this bench scale study due to its lower vapor pressure.

A rotating disk apparatus was designed to reproduce in the laboratory a well-controlled flow field with mass-transfer coefficients of the same order of magnitude as those predicted for fully developed falling liquid film flows encountered during liquid cleaning processes. The rotating disk format was selected for cleaning experiments because the mass-transfer coefficient is essentially uniform across the disk surface, simplifying the subsequent mass-transfer analysis. This experimental arrangement also facilitates rapid changes in the rotation speed that controls the Reynolds number and mass-transfer coefficient. This approach corresponds to a local

Correspondence concerning this article should be addressed to C. S. Grant.
Present addresses of: A. T. Perka, Hoechst-Celanese Corporation, Charlotte, NC; W. D. Thomas, Intel Corp., Phoenix, AZ; and R. Caton, Union Carbide Corp., Cary, NC.

measurement of a cleaning process on a large-scale piece of equipment.

A series of liquid cleanings were performed on melted behenic acid samples with different time-temperature histories (varying degrees of melting) to study the impact of variations in both the morphology and porosity of the behenic acid coatings. A theoretical mass-transfer-based model was developed to describe the amount of residue removed as a function of time, at various rotation speeds (fluid velocity). The theoretical model results were compared to cleaning data from the experimental residue/solvent system under mass-transfer conditions. The role of temperature in the cleaning process was also evaluated experimentally and theoretically.

Theory

Mass-transfer coefficients during solvent cleaning

To develop a mass-transfer model for cleaning, a simplified representation of the cleaning process is used. The results may be extrapolated to the conditions found in a commercial vessel. As a first approximation, the liquid cleaning can be modeled as a falling film of liquid into which the solid residue dissolves. The volume flow of the solvent per unit width of the reactor, Γ , is determined by integrating the velocity distribution over the surface of the reactor:

$$\Gamma = \left[\int_0^W \int_0^\delta v_x dz dy \right] = \frac{g\delta^3}{3\nu}, \quad (1)$$

where v_x is the velocity in the x -direction, W is the width of the reactor, g is the gravitational acceleration, and δ is the liquid film thickness. A Reynolds number based on the average velocity, Re_f , is useful for correlating overall heat- and mass-transfer fluxes (Bird et al., 1960):

$$Re_f = \frac{4 \langle v_x \rangle \delta}{\nu} = \frac{4g\delta^3}{3\nu^2}, \quad (2)$$

where $\langle v_x \rangle$ is the average velocity of a fluid element in the falling film.

The problem of diffusion from a solid surface into a falling film has traditionally been approached by assuming that all resistance to mass transfer occurs in a laminar boundary layer very close to the solid surface. It is also assumed that the flow is fully developed and constant. This approach works well for laminar flow provided that the Schmidt number (Sc) is sufficiently high that the diffusion layer is much thinner than the laminar boundary layer. The average mass-transfer coefficient \bar{k} for a falling film of length L in laminar flow has been determined by several researchers (Kramers and Kreyger, 1956; Iribarne et al., 1967; Oliver and Atherinos, 1968; and Wragg et al., 1968) as

$$\bar{k} = 0.912 \left[\frac{\Gamma g^2 \nu^4}{L^3} \right]^{1/9} Sc^{-2/3}, \quad (3)$$

where L is the distance from the top of the falling film. This equation is reportedly accurate up to an average film Reynolds number of approximately 1,000.

For a vertical falling film, waves form and grow with distance down the wall. Transfer processes in the falling films are dependent on the structure (i.e., amplitude, shape) of the large and small waves in addition to the thickness of the liquid substrate (Dukler, 1959, 1977; Dukler and Bergelin, 1952). The rate of mass transfer in the liquid phase can be enhanced by a factor of 2 when waves are present. In the literature, rippling in falling films has been reported at average film Reynolds numbers as low as 4 (Bird et al., 1960). However, it is generally accepted that the laminar-turbulent transition in falling films occurs roughly between $Re_f = 500$ and 1,000. In the analysis of film condensation on a flat surface a laminar flow solution is used to approximate the case of wavy flow (Whitaker, 1977).

Large-scale stainless-steel reactors are on the order of 2-3 meters in height. At the bottom of the falling film (e.g., at $L = 200$ cm) the calculated value of 530 for the average Reynolds number is in the laminar-turbulent transition region; most of the falling film would be characterized as laminar flow with ripples. Since laminar-flow mass-transfer predictions have been shown to be accurate at Reynolds numbers as high as 1,000 (Kramers and Kreyger, 1956; Oliver and Atherinos, 1968), it is reasonable to use them for prediction of cleaning rates for the behenic acid-ethanol system at a specific point on the surface.

Rotating disk design

The rotating disk apparatus (RDA) used in this work is geometrically similar to the rotating disk electrodes that are widely used in electrochemical studies (Albery and Hitchman, 1971; Levich, 1962). The spinning disk face creates a spiral flow field in which the fluid is drawn axially toward the disk surface and then accelerated radially outward due to centrifugal forces (see Figure 1). One of the key benefits of the rotating disk is that the mass flux in the axial direction is not a function of radial position, and is therefore constant over the entire disk face (Gregory and Riddiford, 1956). This

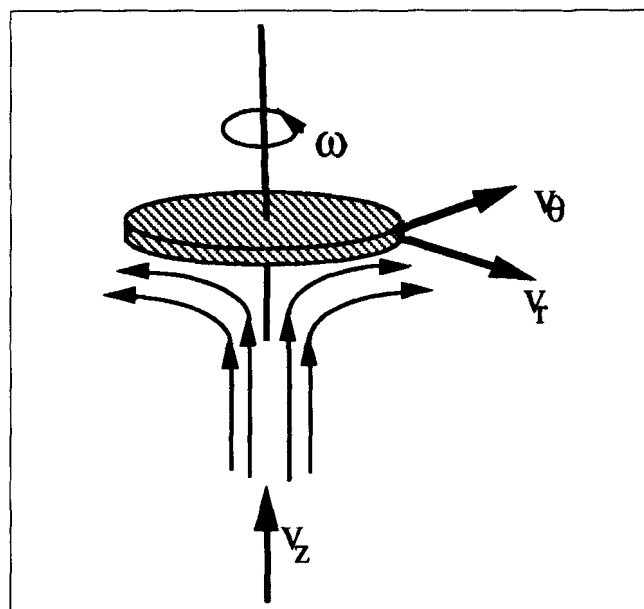


Figure 1. Rotating disk apparatus.

Table 1. Physical Properties of Ethanol and Behenic Acid

Temperature (°C)	52	30	
Temperature (K)	325	303	Notes
<i>Ethanol Physical Properties</i>			
Molecular weight	46.069	46.069	
Density (g/cm ³)	0.789	0.789	At 20°C
Viscosity (cp)	0.68	0.96	At input temperature
Kinematic viscosity (cm ² /s)	8.56E-03	1.22E-02	
Thermal conductivity (W/cm·k)	1.66E-03	1.66E-03	Good at 16–91°C
Heat of vaporization (cal/mol)	9,260	9,260	At normal boiling point
Heat of vaporization (J/g)	841	841	At normal boiling point
Normal B.P. (°C)	78.4	78.4	
Vapor pressure (mm Hg)	243	79	Antoine; good at (–3)–96°C
Liquid Cp (cal/g·°C)	0.660	0.660	Good at 20–80°C
Ideal gas Cp (cal/mol·°C)	15.8	15.8	
Surface tension (dyne/cm)	20.37	21.91	Fit of CRC data at 10–30°C
<i>Behenic Acid Physical Properties</i>			
Molecular weight	340.58	340.58	
Liquid density (g/cm ³)	0.822	0.822	Liquid at 90–100°C
Heat of crystallization (kcal/mol)	188	188	
Normal B.P. (°C)	306.0	306.0	
Melting point (°C)	80	80	
Refractive index	1.427	1.427	Liquid at 100°C

uniformity of the mass flux makes the rotating disk ideal for mass-transfer experiments to simulate the local cleaning behavior at a specific location in a falling liquid film. Variations in the RDA rotation speed correspond to changes in the mass-transfer coefficient. The RDA also enables us to obtain laminar mass-transfer coefficients in the same range as the average \bar{k} for a falling film.

The theory describing the three-dimensional flow field created by a rotating disk is well-defined and has been treated extensively in the literature (Albery and Hitchman, 1971; Levich, 1962). Schlichting (1968) and Newman (1973) both present the numerical solution originally attributed to Cochran (1934). White et al. (1976) reported an improved numerical solution method that generates more accurate values for the characteristic dimensionless groups. Although presented in different forms, Newman (1973) and Albery and Hitchman (1971) both give solutions to the equations for mass transfer in laminar flow that can be rearranged to yield an expression for the rotating disk mass-transfer coefficient, k_R , as a function of the diffusion coefficient, rotation speed, ω , and Schmidt number:

$$k_R = 0.620(D_{AB}\omega)^{1/2} Sc^{-1/6} \quad (4)$$

Mohr and Newman (1975, 1976) report that Eq. 4 is valid up to a disk Reynolds number (Re_d) of 200,000,

$$Re_d = \frac{r^2\omega}{\nu} \quad (5)$$

where r is the disk radius.

The initial RDA rotation speed was chosen here by evaluating the falling-film mass-transfer coefficient predicted by Eq. 3 at a specific location on a reactor surface and equating it to the k_R in Eq. 4. The value of ω for the rotating disk experiment was then calculated using Eq. 4. Physical properties of ethanol and behenic acid are in Table 1 (Reid et al., 1977). For example, the dissolution of behenic acid into a falling film of ethanol the mass-transfer coefficient, at a point located 100 cm from the top of the reactor, would be 9.16×10^{-6} cm/s (Table 2); the corresponding value of ω was 32 rpm.

In the study of the rotating disk apparatus, the effects of the edge of the disk on the hydrodynamic mass transport of material to and from the disk surface have not been precisely quantified. Levich (1962) has shown that the thickness of the diffusion boundary layer at the disk surface is given by

$$\delta' = 0.5(\delta_0) \left(\frac{D_{AB}}{\nu} \right)^{1/3} \quad (6)$$

where D_{AB} is the diffusion coefficient of solute in solvent, ν is the kinematic viscosity of solvent, and δ_0 is the hydrody-

Table 2. Summary of Falling-Film Mass-Transfer Coefficient Calculations

Parameter	Value	Description
Wall location, x	100 cm	Distance from top of reactor
Avg. film temp. ($T_i + T_s$)/2	52°C	For ethanol, wall temp. 25°C and condensation temp. 78°C
Diffusion coeff., D_{AB}	7.0×10^{-6} cm ² /s	Evaluated at 52°C from Wilke–Chang model
Film thickness, $\delta(x)$	0.026 cm	At $x = 100$ cm
Flow per unit width, Γ	0.677 cm ² /s	At $x = 100$ cm, Eq. 1
Reynolds No., Re	316	At 52°C
Schmidt No., Sc	1,223	At 52°C
Mass-transfer coeff.	9.16×10^{-4} cm/s	At 52°C, Eq. 3
RDA rotation speed	32 rpm	Corresponding to mass-transfer coefficient. Eq. 4

dynamic boundary layer thickness. The hydrodynamic boundary layer thickness is represented as:

$$\delta_0 = 3.6 \left(\frac{\nu}{\omega} \right)^{0.5} \quad (7)$$

In the equations that enable theoretical prediction of the mass transport of materials to and from the disk surface, a series solution for the component of the fluid velocity in the axial direction, v_y , can be generated (Levich, 1962; Newman, 1973; Schlichting, 1968; White et al., 1976). If the diffusion boundary layer thickness, δ' , is significantly less than the hydrodynamic boundary layer thickness, δ_0 , [$(\delta'/\delta_0) < 0.05$], this series solution may be truncated after the first term (Levich, 1962). Inclusion of the higher order terms results in corrections that give a mass flux to or from the disk, which is on the order of 3 to 5% larger than that found when the higher order terms are ignored. These higher order terms can be used to predict effects of the edge of the disk on the mass transport to and from the disk surface, as the edge effect is believed to extend over the disk to a distance on the order of δ_0 .

Mass-transfer development

A theoretical equation for the liquid cleaning can be written based on the mass transfer of behenic acid. The rate of removal of behenic acid from the rotating disk may be computed in terms of the rotating disk mass-transfer coefficient and the concentration driving force:

$$\frac{dM_{BAC}}{dt} = -k_R A (C_{BAC,S} - C_{BAC}), \quad (8)$$

where M_{BAC} is the mass of behenic acid remaining on the disk, $C_{BAC,S}$ is equal to the concentration of behenic acid in ethanol at the solid-liquid interface, C_{BAC} is the concentration of behenic acid in the bulk solution, A is the cross-sectional area of the disk, and k_R is the mass-transfer coefficient. The initial condition is

$$C_{BAC} = 0 \text{ @ } t = 0, \quad (9)$$

with

$$\left(\frac{M_{BAC,0} - M_{BAC}}{V} \right) = C_{BAC}, \quad (10)$$

where V is the volume of the solution and $M_{BAC,0}$ is the initial mass of behenic acid on the disk. Integrating yields

$$(M_{BAC} - M_{BAC,0}) = VC_{BAC,S}(e^{-k_R A t/V} - 1). \quad (11)$$

At short times ($t \rightarrow 0$) the mass remaining on the disk can be

$$M_{BAC} = M_{BAC,0} - (k_R A C_{BAC,S})t. \quad (12)$$

In this study the cleaning data are reported as the fraction of behenic acid removed from the surface, f_r , as a function of

time. For the rotating disk mass-transfer coefficient (Eq. 4) the fraction removed f_r is defined as

$$f_r = 1 - \frac{M_{BAC}}{M_{BAC,0}} = \frac{k_R A C_{BAC,S} t}{M_{BAC,0}} = \frac{[0.620(D_{AB}\omega)^{1/2} Sc^{-1/6}] C_{BAC,S} A t}{M_{BAC,0}} \quad (13)$$

It is assumed that $C_{BAC,S}$ is equal to the saturation concentration of behenic acid in ethanol at the liquid cleaning temperature. Thus, the model predicts that in an ideal system the removal at short times will vary linearly with cleaning time, and with the square root of the rotation speed.

Incorporating the theoretical expression for the falling-film mass-transfer coefficient (Eq. 3), the fraction removed can be

$$f_r = \frac{(0.912[\Gamma g^2 \nu^4 / L^3]^{1/9} Sc^{-2/3}) C_{BAC,S} A t}{M_{BAC,0}}. \quad (14)$$

It may be possible to evaluate an experimental value of the volume flow per unit length of reactor surface. It would be difficult, however, to experimentally measure the fraction removed at a specific location L on the reactor surface.

Experimental Studies

Design of experiments

The apparatus for the liquid cleaning experiments is shown in Figure 2. A lab stirrer (Fisher Sted-Fast; model SL 600) with a range of 30 to 600 rpm was used to drive the rotating disk. An optical tachometer was used to calibrate the stirrer and to verify each change in rotation speed. The stirrer design permitted the threaded motor shaft to be moved vertically through the chuck, permitting easy submersion and withdrawal of the test sample from the cleaning solvent. The jar containing the cleaning solvent was placed in a Lauda model MS-6 constant temperature bath and held by a wire cage; this kept the jar in a steady, reproducible position for the liquid cleaning experiments. A Troemner model 700 submersible magnetic stirrer allowed agitation of the cleaning solvent during prerun temperature equilibration. The temperature of the liquid cleaning solvent was monitored using a multichannel digital thermocouple.

Because the mass-transfer coefficient for a rotating disk is independent of the disk radius, any convenient radius may be chosen so long as the disk Reynolds number does not exceed the range over which the equation for k_R is valid. A disk radius of 9 mm was chosen because it was large enough to hold a sufficient residue loading for gravimetric analysis.

For the rotation velocities and the disk size used in this study δ'/δ_0 was equal to 0.047, so that the higher order terms in the expression for v_y could be omitted for the experiments reported in this article. However, the value of δ_0 ranges from 30% to 50% of the disk radius, creating the possibility that the edge effect altered the transport of fluid to and from the disk surface.

In a study of the effect of radial diffusion on the mass-transfer rate in electrochemical studies using a rotating disk

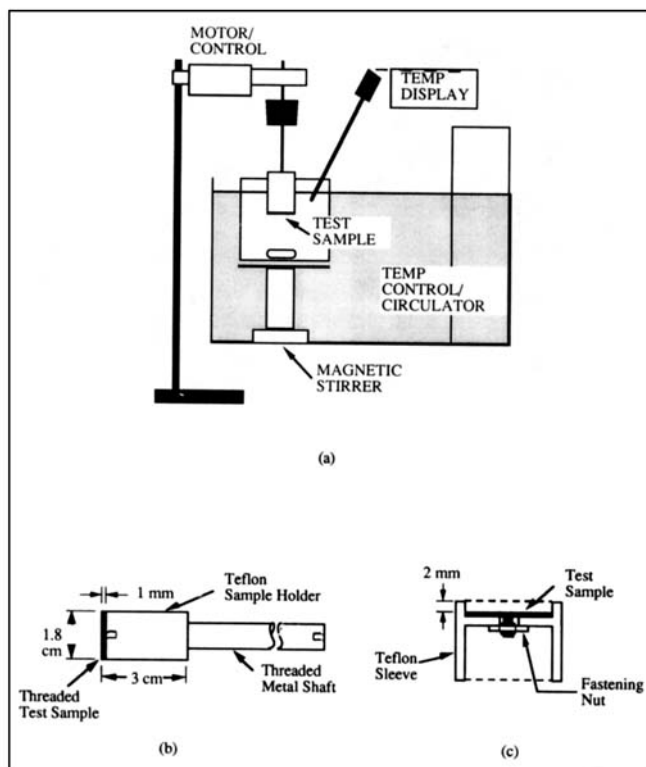


Figure 2. (a) Benchtop setup for liquid cleaning experiments; (b) test sample holder; (c) sample coating sleeve.

electrode, Smyrl and Newman developed the following correction to the Levich equation (Smyrl and Newman, 1971):

$$\frac{I_{\text{lim}}}{I_{\text{Levich}}} = 1 + \frac{1.9193}{Sc^{1/2} Re^{3/4}}, \quad (15)$$

where I_{lim} is the limiting current on a rotating disk electrode when radial diffusion is accounted for, and I_{Levich} is the diffusion-layer solution for the total current to the electrode. At 30 rpm (the lowest rotation speed used in this study), the ratio for our experimental system is 1.0007. Hence, the error due to edge effects was assumed to be negligible for the current system.

The theoretical development of the average k -value assumes that the diffusion layer is much smaller than the laminar boundary layer for high Sc numbers. For the range of rotation speeds studied, the lowest Sc -value was 1269, supporting the assumption of a small diffusion layer.

Behenic acid sample preparation and preparation of cleaning samples

In this study, liquid scintillation is used to determine the amount of behenic acid removed from the rotating disk. This analytical technique requires the stock behenic acid (Eastman Chemical Company) to be mixed with ^{14}C labeled behenic acid. Behenic Acid-Carboxy- ^{14}C (specific activity 16.1 mCi/mmol) was obtained from Sigma Chemical Company. The manufacturer reported a purity of 98% based on high-performance liquid chromatography (HPLC) analysis. Thin-

layer chromatography (TLC) analysis on silica gel plates with a 49:1 ethyl acetate to acetic acid solvent produced a single band with an R_f value of 0.85.

The ^{14}C behenic acid powder (2.7 mg) was added to a slurry of unlabeled behenic acid powder (45 g) and ethanol (451 g). In order to create a uniform behenic acid mixture the slurry was heated and stirred at 60°C in a constant water bath until the crystals completely dissolved. The solution was then cooled to 25°C, producing behenic acid crystals. The crystals were vacuum filtered and placed in an oven at 38°C for 20 hours to remove excess ethanol. The dried crystals were crushed into a powder; the resulting radioactive mixture was combined with ethanol for solubility studies. TLC analysis of the labeled and unlabeled behenic acid mixture using the aforementioned plate-solvent system resulted in a single band with an R_f value of 0.85.

The test substrates were unpolished, mill finish type 304 stainless steel that had been sandblasted with coarse grit. The rough finish was intended to resemble the unpolished stainless-steel surfaces typically found in many chemical processing vessels. Prior to the application of a behenic acid coating, the stainless-steel samples were cleaned with ethanol and a test tube brush. After scrubbing, the samples were wiped off with a clean Kimwipe, soaked in ethanol, and allowed to dry. After weighing, the samples were placed into Teflon sample coating sleeves and fastened with a nut (Figure 2b).

The stainless-steel samples were coated with a 10% (by weight) behenic acid/ethanol slurry. To make the slurry, behenic acid powder mixture was mixed with HPLC-grade ethanol, heated on a hot plate stirrer to dissolve the behenic acid, and slowly cooled to 25°C with stirring. The Teflon sleeves containing the stainless-steel test samples were then each filled with 500 μL of the cooled slurry using a digital pipette. The time-temperature history of the coatings is defined by the melting process. In initial studies, the samples were baked for approximately 16 to 18 minutes, until they developed a "sintered" appearance, that is, no longer flaky, but not completely melted. After baking, the samples were removed from the oven, allowed to cool to room temperature and weighed. The average weight of the sintered samples was 35.7 \pm 4.8 mg. For "melted" samples, the bake time was increased to 20–21 min, which caused the behenic acid to melt into a clear liquid; "melted" samples had a hard, waxy-crystalline appearance with no visible porosity. The average weight of the melted samples was 31.0 \pm 2.2 mg.

Solubility studies

The saturation concentration of the behenic acid in ethanol, $C_{BAC,S}$, at the liquid cleaning temperature was determined using a liquid scintillation technique. Radiolabeled behenic acid and ethanol were mixed in a glass jar and placed in a constant temperature water bath. The solubility experiments were carried out over a temperature range from 25°C to 62°C. The solutions were allowed to come to equilibrium overnight for a minimum of 16 to 18 hours. Following centrifugation, a 1-mL sample of the supernatant was placed in 10 mL of Cyto Scint Liquid Scintillation Cocktail (ICN, Research Products) and analyzed using a liquid scintillation analyzer (1500 Tri-Carb; Packard Instrument Company).

Liquid cleaning

To perform a liquid cleaning experiment, 100 mL (79 g) of ethanol was weighed into a glass jar and preheated to the liquid cleaning temperature in the constant temperature bath. When the cleaning solvent reached the desired temperature (i.e., 30–50°C) the sample holder coated with behenic acid was attached to the stirrer shaft (see Figure 2), lowered into the cleaning solvent, and the motor and timer were immediately started. The amount of behenic acid removed from the disks was determined by liquid scintillation analysis of the cleaning solvent. The ethanol sample was placed in a scintillation vial and mixed with Cyto Scint prior to counting.

At the end of the run the disk was placed in the ethanol, which was heated to 60°C to remove any remaining behenic acid. The resulting solvent was counted in order to determine the total amount of behenic acid originally on the disk. The fraction of behenic acid removed, f_r , was calculated by recording the raw counts from the liquid scintillation measurement and dividing by the total counts at the end of the run. The fraction removed was corrected for volume changes due to sampling. The disk was also weighed at the end of the run to close the mass balance on the system.

Results and Discussion

Solubility studies

Domanska (1987) determined the solubility of behenic acid in a number of one-component solvents (e.g., ethanol, methanol) by a dynamic method developed by Buchowski et al. (1975). In this method mixtures of solute and solvent were heated at a slow rate with continuous stirring. The temperature at which all of the crystals disappeared was defined as the temperature of solution. A comparison of the solubility values from our liquid scintillation studies in ethanol to the literature values reported by Domanska (1987) indicate good agreement in the temperature range of the liquid cleaning studies (Figure 3). Our experimentally determined solubility values were utilized in the mass-transfer model.

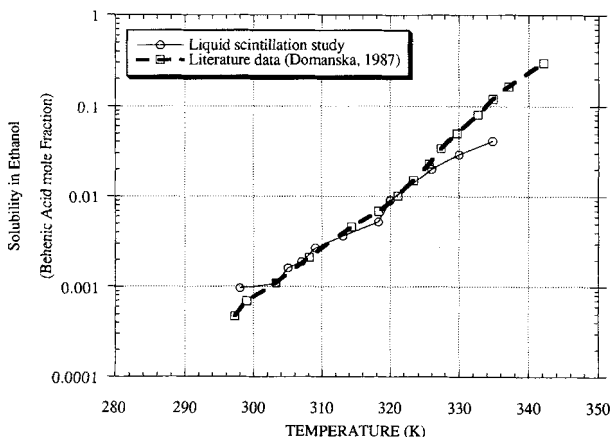


Figure 3. Comparison of experimental solubility determined by liquid scintillation to literature solubility values determined by dynamic technique (Domanska, 1987).

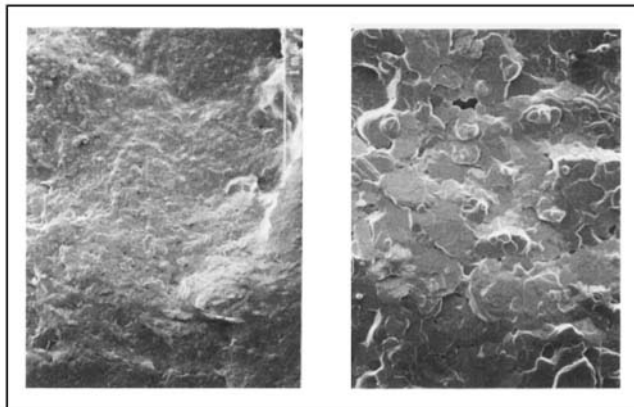


Figure 4. Scanning electron micrograph of melted behenic acid coating on stainless-steel disk (a) 40X magnification (b) 400X magnification.

Physical characteristics of melted and sintered samples

When the coated samples are taken out of the oven, the surface area of the disk is exposed to a nonuniform temperature gradient and therefore the cooling rate across the disk is not uniform. According to Askeland (1989), during crystallization once a solid nucleus forms, the rate at which the nucleus grows during solidification depends on the manner in which heat is removed from the solid-liquid system. Specifically, the manner in which the latent heat of fusion is removed determines the growth rate and final structure of the substance. Rapid cooling of the melted phase prevents crystal growth. Scanning electron micrographs of the “melted” samples in our research, shown in Figure 4, reveal a relatively smooth surface showing sparsely distributed pores from 10 to 25 μm in diameter. In contrast, the sintered samples showed signs of dendrite growth when completely cooled. The sintered micrographs indicate a very flaky structure with pores as large as 1 mm by 0.5 mm (Figure 5). Upon further magnification, the flakes appear to have the same surface structure as the melted samples.

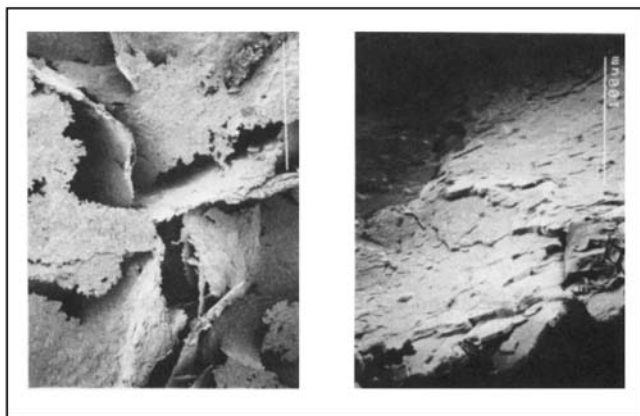


Figure 5. Scanning electron micrograph of sintered behenic acid coating on stainless-steel disk (a) 40X magnification (b) 400X magnification.

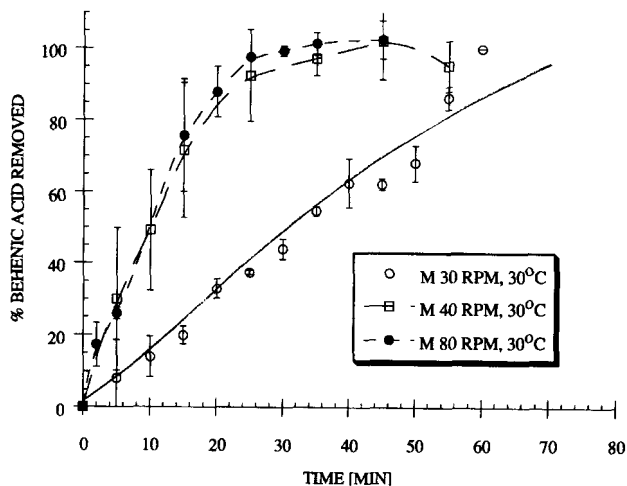


Figure 6. Liquid cleaning of melted samples at 30°C; varying rotation speed.

Liquid cleaning results

Liquid cleaning experiments were conducted at temperatures ranging from 30°C to 50°C; the rotation speeds ranged from 30 rpm to 80 rpm (the corresponding mass-transfer coefficients range from 6.4×10^{-4} cm/s to 1.2×10^{-3} cm/s). The results from the liquid cleaning experiments are presented in Figures 6 to 13 as the percentage of behenic acid removed vs. cleaning time. Each curve represents the average of two cleaning experiments; any data above 100% is due to the scatter associated with the liquid scintillation measurements. The error bars represent $\pm\sigma$ of the average. The experimental cleaning rates are analyzed in the following groups: (a) constant temperature at varying rpm, (b) constant rpm and varying temperature, and (c) sintered vs. melted samples.

At the lowest temperature in this study (30°C), as the rotation speed increased from 30 rpm to 80 rpm the rate of removal increased significantly for both the melted and sintered samples (Figures 6 and 7). It should be noted that there is not a clear trend for the changes with rotation speed in

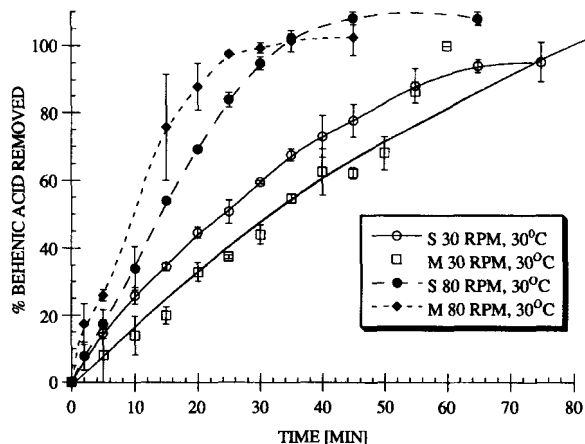


Figure 8. Comparison of melted and sintered samples at 30°C; high and low rotation speeds.

either case. Figure 8, however, indicates that there are variations in the removal characteristics of the melted and sintered samples. This may be due to differences in the initial structure and morphology of the coatings. Figures 9 and 10 illustrate that at a higher temperature (40°C) there is only a slight change in the rate as the rotation speed is varied from 30 to 80 rpm. These results are independent of the time-temperature history of the samples.

The temperature dependence of the cleaning process at 30 rpm is presented in Figures 11 and 12. At higher temperatures (up to 50°C) both the melted and sintered behenic acid is removed from the stainless steel at a high rate; 100% removal in 10-15 min at 50°C as compared to 50 to 60 minutes for samples cleaned at 30°C. Similar trends are observed for both sintered and melted samples. At 50°C, the time-temperature history of the samples does not play a significant role in the cleaning rate (Figure 13). In this instance, the temperature dependence appears to be the dominant parameter controlling the removal of behenic acid. This temperature effect is discussed in detail later in this article.

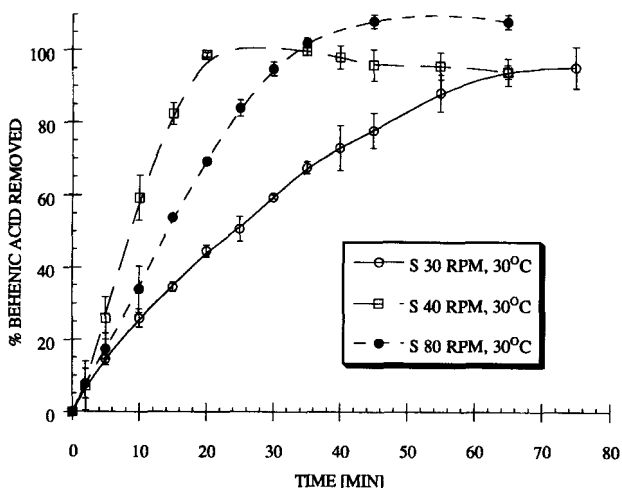


Figure 7. Liquid cleaning of sintered samples at 30°C; varying rotation speed.

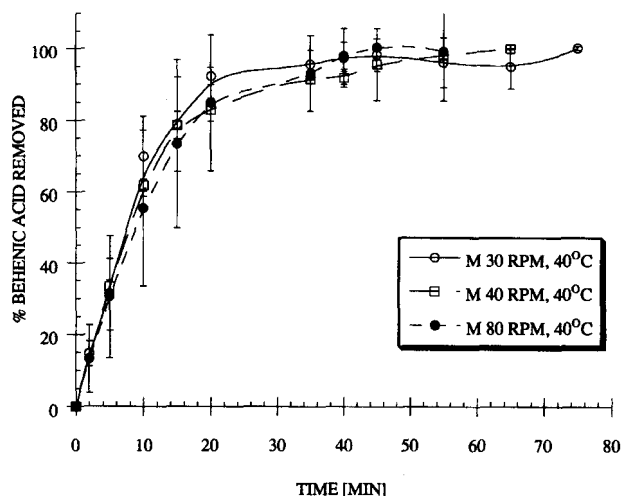


Figure 9. Melted samples; liquid cleaning at 40°C; varying rotation speeds.

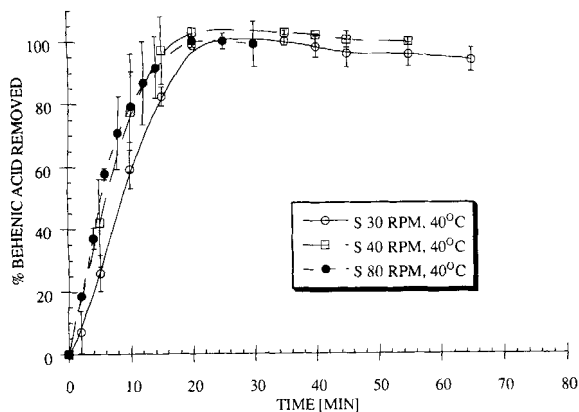


Figure 10. Liquid cleaning of sintered samples at 40°C; effect of increasing rotation speed.

Comparison of initial cleaning rates to mass-transfer model

There are three assumptions associated with the mass-transfer model used for comparison with experimental data: (1) a perfectly smooth, flat residue surface with an area equal to the area of the stainless-steel rotating disk used in the experiments, (2) a concentration of behenic acid at the solid-liquid interface equal to the saturation concentration of behenic acid in ethanol at a specific temperature, and (3) the removal of behenic acid occurs via diffusion of individual residue molecules.

The theoretical cleaning curve was evaluated from Eq. 13 using the initial weight of the behenic acid sample coating. The initial experimental cleaning rate can be determined from the slope of the experimental curve at short cleaning times (linear portion). Figures 14 and 15 show examples of experimental and theoretical cleaning for sintered and melted samples. Note that the difference between the theoretical curves for two experiments conducted under similar conditions is the initial weight of the sample, $M_{BAC,0}$. In some instances, there is good agreement between the rate predicted by the RDA mass-transfer model in Eq. 13 and the initial experimental cleaning rate. There are, however, a number of cases where

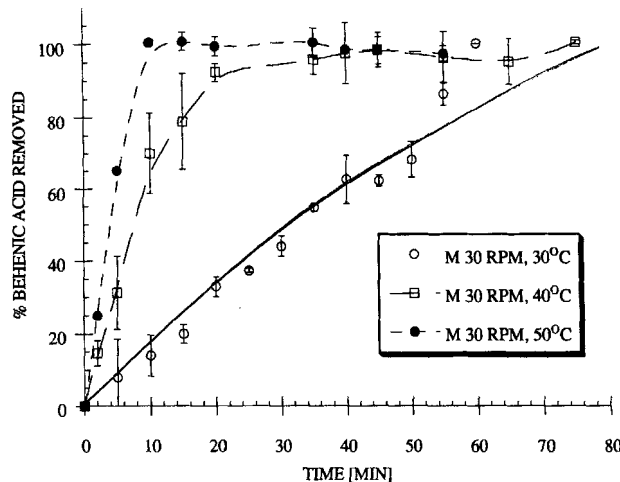


Figure 12. Melted samples cleaned at 30 rpm and increasing temperature.

the theoretical model deviates significantly from the experimental data. As shown in Figure 16, at 30 rpm and 30°C the model overpredicts the rate of behenic acid removal for melted samples at long times. There is also a slight deviation between the experimental and theoretical data for the melted samples cleaned at 40°C and 50°C. The melted samples produce coatings that are, generally speaking, more tenacious, possibly due to an increase in the bond strength during melting. This may result in a variation in the dissolution of the behenic acid. In contrast, at 40 rpm and 30°C, the theory underpredicts the observed experimental cleaning rate for both sintered and melted samples (Figures 17 and 18).

According to the Levich theory, the k -value should vary linearly with $\omega^{1/2}$. The expectation of a clear trend in the rotational speed dependence was not found. When the data were plotted as the experimentally determined value of the rate of removal vs. $\omega^{1/2}$, a linear relationship was not obtained (Figure 19). This initial expectation was based on the behenic acid coating behaving like an ideal system. Some of the scatter in the data also limits the ability to see clear trends in the cleaning behavior.

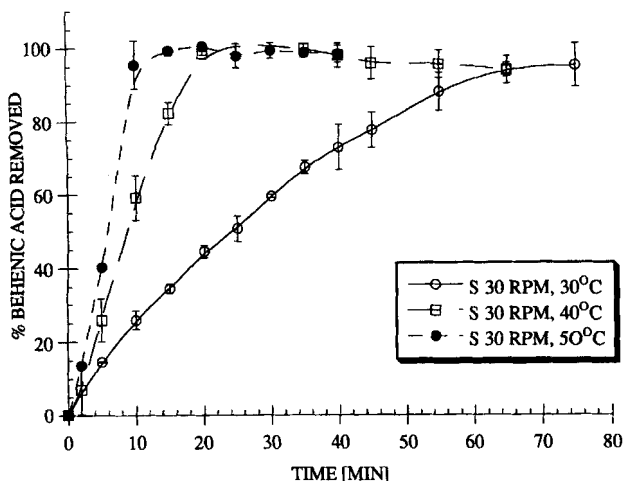


Figure 11. Role of temperature in cleaning of sintered samples at 30 rpm.

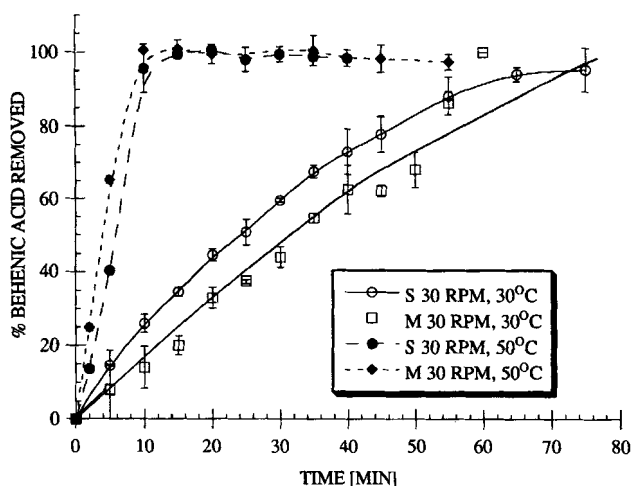


Figure 13. Sintered vs. melted samples cleaning at 50°C, at high and low rotation speeds.

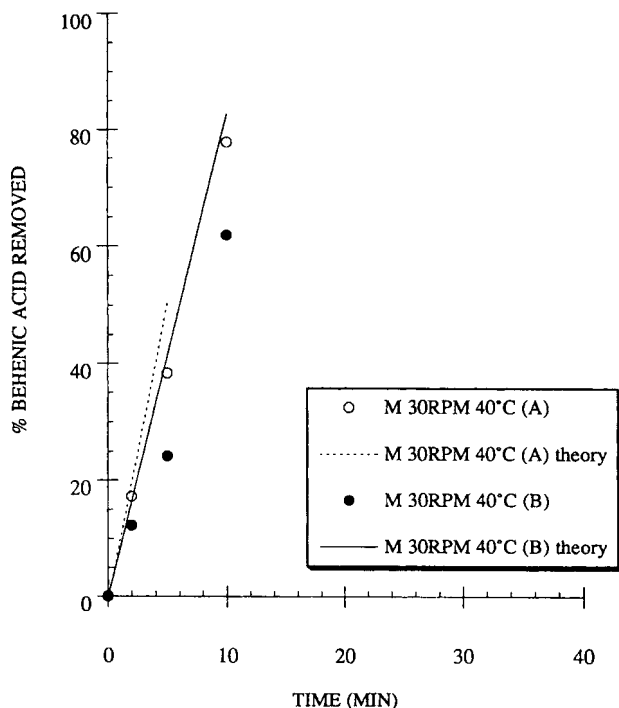


Figure 14. Experimental results vs. RDA mass-transfer model (Eq. 13) for melted samples cleaned at 30 rpm and 40°C.

A and B designate the two repeat runs under the same conditions.

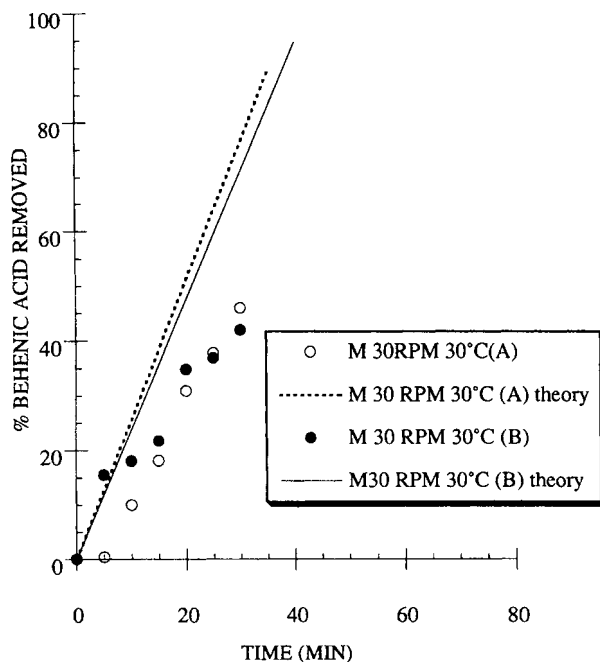


Figure 16. Experimental results vs. RDA mass-transfer model (Eq. 13) for melted samples cleaned at 30 rpm and 30°C.

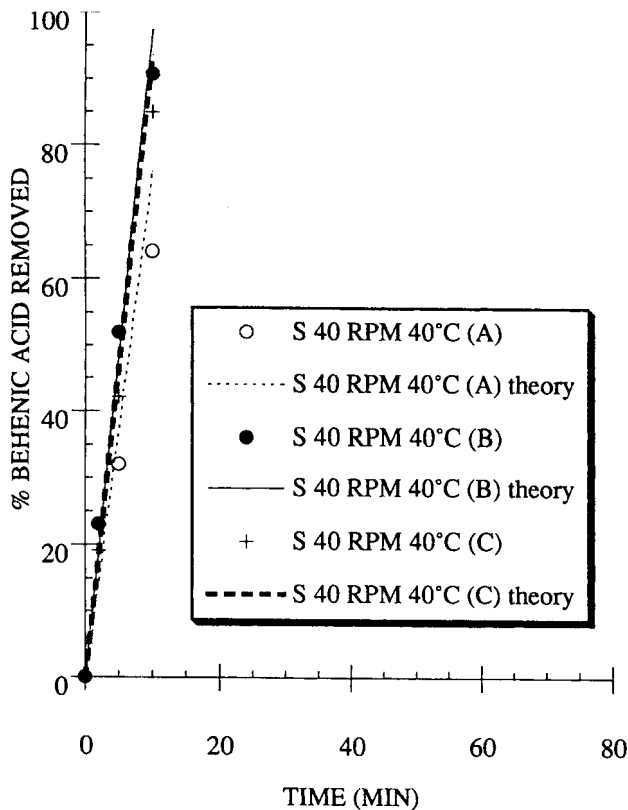


Figure 15. Experimental results vs. RDA mass-transfer model (Eq. 13) for sintered samples cleaned at 40 rpm and 40°C.

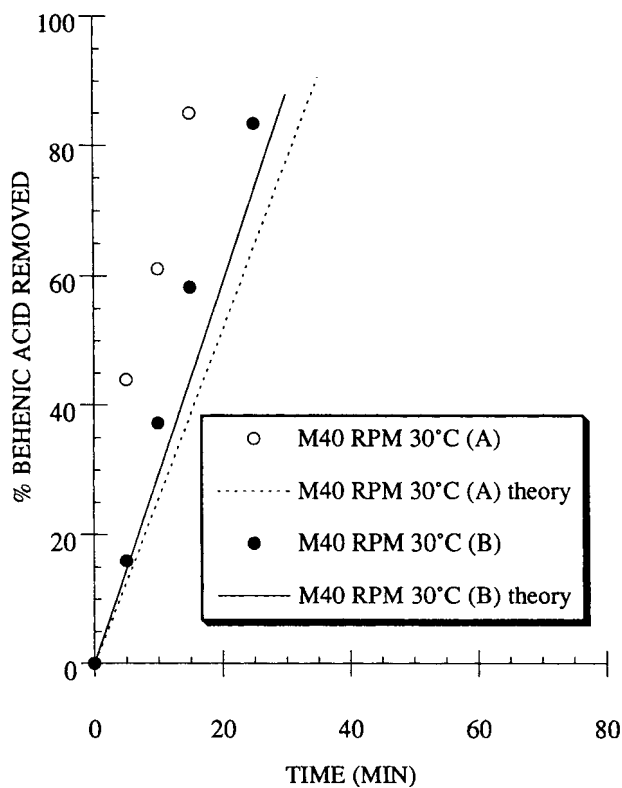


Figure 17. Experimental results vs. RDA mass-transfer model (Eq. 13) for melted samples cleaned at 40 rpm and 30°C.

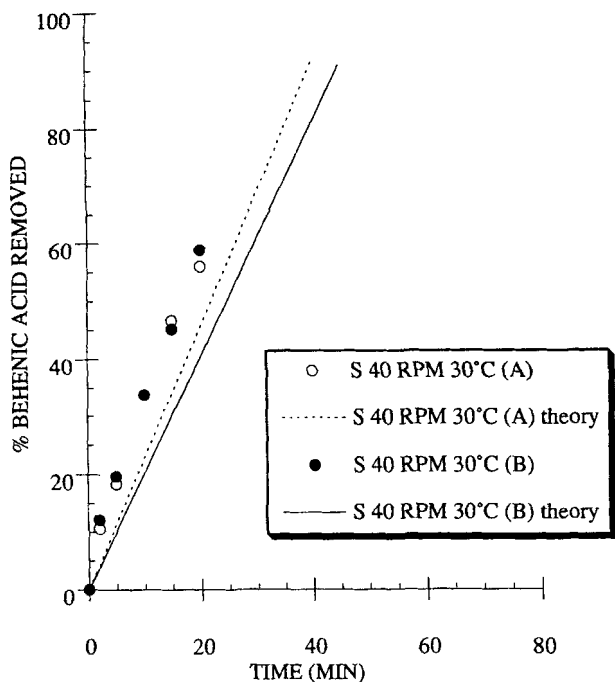


Figure 18. Experimental results vs. RDA mass-transfer model (Eq. 13) for sintered samples cleaned at 40 rpm and 30°C.

There are a number of reasons why the mass-transfer model does not accurately predict what occurs in the behenic acid cleaning process. Possible explanations for the deviation from the theoretical model include variations in the estimated diffusion coefficient and an error in the predicted value of the concentration driving force for mass transfer. In addition, the scanning electron micrographs reveal that the behenic acid layer has a rough surface and significant porosity, both of which may change the surface area available for mass transfer. Therefore, the assumed surface area used in the mass-transfer model predictions may change, contributing to the difference between the observed and predicted behenic acid cleaning rates.

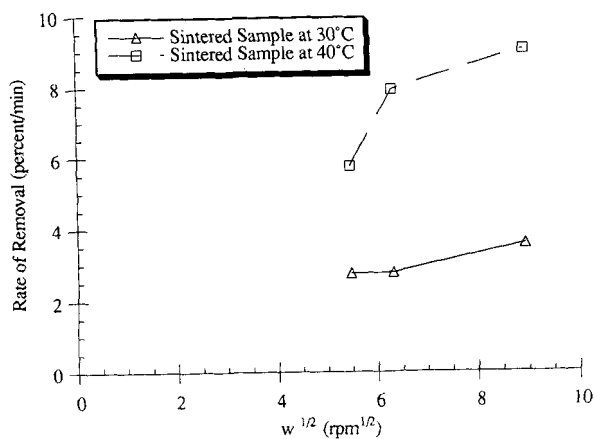


Figure 19. Removal rate vs. $\omega^{1/2}$ for sintered samples at 30 and 40°C.

These results suggest that the removal of the behenic acid is not due solely to a simple molecular dissolution mechanism. One explanation for this behavior is that the connections between the individual crystal structures observed in the electron micrographs may be nonuniformly dissolved by the ethanol. If this occurs, then entire crystals or parts of crystals may be removed as aggregates. This behavior was observed in previous experiments in which the percentage of behenic acid removed was determined gravimetrically (the samples were removed from the ethanol after cleaning for a set time period and weighed). When the test samples were removed from the ethanol, nonuniform bare patches of stainless steel were observed after approximately 60% of the sample was cleaned. This removal of large behenic acid crystals may result in rates that are higher than those predicted by the mass-transfer model. At longer cleaning times, the presence of bare patches, however, invalidates the assumption that the area of the behenic acid coating available for mass transfer is equal to the entire area of the stainless-steel disk.

The mass-transfer model also assumes that diffusion takes place only between the behenic acid layer and the ethanol interface, that is, the behenic acid is soluble in ethanol, but the ethanol is insoluble in the behenic acid layer. Visual inspection of partially cleaned test samples reveals behenic acid patches with a spongy appearance reminiscent of solvent swelling in some polymers. This observation provides evidence that the assumption of ethanol insolubility in the behenic acid layer may be in error. If the ethanol does dissolve into the behenic acid layer, then a mechanism other than simple mass transfer from the surface must account for the cleaning of this system.

Again, the surface roughness may be a contributing factor. It is well known that for other flow geometries (e.g., flow in a pipe), a small amount of surface roughness dramatically reduces the Reynolds number corresponding to the transition from laminar to turbulent flow. In an analogous manner, the surface roughness of the coated RDA (not the substrate morphology) may be creating turbulence that enhances mass transfer that is not accounted for in the laminar RDA mass-transfer model. In summary, the simple mass-transfer theory proposed here does not predict the rate of removal under the conditions presented in this study. It does, however, qualitatively predict the trends in rotation speed and temperature in limited cases.

Temperature effects

The experimental data do not appear to behave in a manner that can be predicted by a simple mass-transfer model. There appears to be, however, a large dependence on the temperature of the cleaning solvent. At low temperatures (e.g., 30°C), there is a large variation in the initial rate of removal with rotation speed for sintered samples. This suggests that at this temperature the removal is mass transfer controlled. At higher temperatures (e.g., 40 and 50°C), however, the rotation speed does not significantly change the initial rate of removal. This high-temperature behavior may be due to the thermal loosening of the behenic acid film and/or thermal stresses in the coating. This thermal dependence can be explained by determining the temperature dependence of the rate of removal of the behenic acid from the rotating

disk. Using the data on the rate of removal at different temperatures, an activation energy of removal can be evaluated using an equation of the following form (Hill, 1977):

$$R(T) = R_0 e^{-E_a/RT} \quad \text{or} \quad \ln[R(T)] = \ln R_0 - \frac{E_a}{RT}, \quad (15)$$

where $R(T)$ is the temperature-dependent experimental rate of removal, E_a is the activation energy, T is the absolute temperature, R is the gas constant, and R_0 is a preexponential factor (a constant). Reactions with high activation energies are considered very temperature sensitive; those with low activation energies are relatively temperature insensitive (Levenspiel, 1972). The flux of behenic acid to the surface, N_A , can be generally described in terms of the rates of adsorption and desorption as follows:

$$N_A = k_m(C_b - C_s) = k' C_s - \hat{k}, \quad (16)$$

where \hat{k} is the rate of desorption of material from the surface, C_s is the surface concentration, C_b is the bulk concentration, k' is a rate constant, k_m is the mass-transfer coefficient, and $k' C_s$ is the rate of adsorption of material to the surface. The surface concentration in terms of the adsorption and desorption terms becomes

$$C_s = \frac{\hat{k} + k_m C_b}{(k_m + k')}. \quad (17)$$

Rewriting the flux in terms of the new C_s expression yields

$$(C_b - C_s) = C_b - \left(\frac{\hat{k} + k_m C_b}{(k_m + k')} \right). \quad (18)$$

Simplifying this expression yields

$$(C_b - C_s) = \frac{C_b K - 1}{(k_m/\hat{k}) + K}, \quad (19)$$

where K is defined as the inverse solubility. This is a ratio of the rates of adsorption and desorption:

$$K(T) = \frac{k'}{\hat{k}} = \frac{1}{S(T)} \quad (20)$$

and S is the solubility. It should be noted that both K and S are strong functions of temperature. Substituting into the original flux equation results in the following equation:

$$N_A = k_m(C_b - C_s) = k_m \left(\frac{C_b - S(T)}{[S(T)(k_m/\hat{k}) + 1]} \right) \quad (21)$$

Taking the natural log of both sides yields

$$\ln N_A = \ln k_m + \ln \left(\frac{C_b - S(T)}{[S(T)(k_m/\hat{k}) + 1]} \right) \quad (22)$$

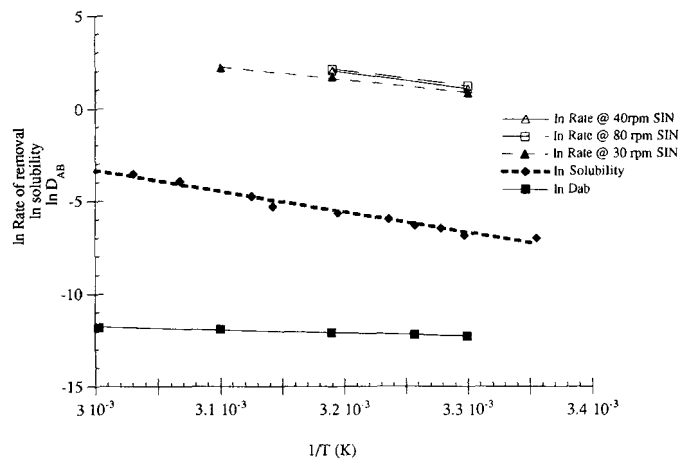


Figure 20. Activation energies for sintered samples based on the data of experimental cleaning rate, solubility, and diffusion coefficient.

Hence, the flux of the behenic acid from the surface can be defined as two terms. The first term represents the contribution due to diffusion and the second term is a solubility term. Both terms are a function of temperature. The next step is to evaluate the role of temperature in the diffusion and the solubility contributions to the overall removal rate.

If the experimental rate of removal and the solubility are plotted as a function of $1/T$, the slope of the resulting plot represents an “activation energy” or a form of E_a (see Eq. 15). A semilog plot of the experimental solubility vs. $1/T$ results in an activation energy of 92 kJ/mol (Figure 20).

To evaluate the role of temperature in the diffusion part of the flux expression, the temperature dependence of the diffusion coefficient was also determined. Figure 20 shows that the E_a value from $\ln D_{AB}$ vs. $1/T$ plot is 13.5 kJ/mol. For sintered behenic acid studies the values of the resulting experimental activation energies are presented in Table 3. If the slope (or E_a) for the reaction rate is the same order of magnitude as the solubility for the different rotation speeds, then the temperature and not the rotation speed controls the removal rates. For example, for the sintered samples the activation energies range from 55.6 to 67.3 kJ/mol for rotation speeds of 30 rpm to 80 rpm, respectively. This analysis indicates that the experimental E_a 's are the same order of magnitude as the solubility; hence, at high temperatures, the temperature controls the total flux or the rate of removal. At low temperatures, the rate is partially diffusion limited because of the dependence of the rate on rotation speed.

Table 3. Summary of Activation Energies, E_A Values: Results of plot of \ln rate vs. $1/T$

Parameter	E_A (J/mol)
Sintered: 30 rpm	55,584
Sintered: 40 rpm	71,616
Sintered: 80 rpm	67,311
Solubility	91,978
Diffusion (D_{AB})	13,531

Summary

The purpose of this work was to investigate the cleaning behavior of an organic coating similar to residues found in stainless-steel chemical reactors. The differences in the degree of sample melting represented the variation in the time-temperature history of the residues at different locations in the reactor (different degrees of residue "bake-on" during processing). The rotating disk was found to be a useful tool for study of the liquid cleaning process. Rotation speeds were selected to produce mass-transfer coefficients in the range predicted for the dissolution of behenic acid into a falling film of ethanol.

A simple mass-transfer model was proposed to describe the removal of behenic acid from stainless steel using RDA. However, the dissolution-based mass-transfer model did not accurately predict the experimental data in all cases. The deviation from theory may be due to the porosity/morphology of the behenic acid layer on the test samples and the removal of large clusters of behenic acid crystals, which results in bare patches on the substrate.

Although the temperature range in this study was only 20°C, there was a significant difference in the cleaning results at 30 and 50°C. At the lowest temperature, the system exhibited the expected trends in cleaning behavior; as the rpm increased, the rate of removal also increased. Under these conditions, the cleaning rate appears to be a function of the transport of bulk solvent to the solid-liquid interface.

In contrast, under certain conditions (e.g., high temperatures) the removal of the coating is almost instantaneous; and the rotation speed does not have a bearing on the removal at high temperatures. A plausible explanation is suggested by the comparison of the temperature dependence of the solubility and the removal rates. In fact, we have seen that the activation energy associated with the removal rate is the same order of magnitude as the solubility E_a value. An understanding of the contribution of the diffusion and the temperature to the removal rate is essential to achieving a full understanding of liquid cleaning mechanisms. The behavior of the porous behenic acid/ethanol system, however, requires a more detailed accounting of the factors governing mass transfer (e.g., solution nonidealities, surface roughness, solvent penetration) in order to accurately predict cleaning rates.

Acknowledgments

This research was supported in part by the EPA Center for Waste Minimization and Management, the Center for Process Improvement and Pollution Prevention, and Dow Chemical Company. We acknowledge technical interactions with Eastman Chemical Company. The authors would like to thank M. Britt for experimental assistance.

Literature Cited

- Albery, W. J., and M. L. Hitchman, *Ring Disk Electrodes*, Clarendon Press, Oxford (1971).
- Anderson, R. M., J. J. Satanek, and J. C. Harris, "Removal of Fatty Soil from Glass-Solvent System Mechanism," *J. Amer. Oil Chem. Soc.*, **36**, 286 (1959).
- Anderson, R. M., J. J. Satanek, and J. C. Harris, "Removal of Fatty Soil from Glass. Electrolyte Detergent-Builder Effect," *J. Amer. Oil Chem. Soc.*, **37**, 119 (1960).
- Askeland, D. R., *The Science and Engineering of Materials*, 2nd ed., PWS-KENT, Boston (1989).
- Bird, R. B., W. E. Stewart, and E. N. Lightfoot, *Transport Phenomena*, Wiley, New York (1960).
- Buchowski, H., W. Jodziewicz, R. Milek, W. Ufnalski, and A.

- Maczynski, "Solubility and Hydrogen Bonding. Part I. Solubility of 4-Nitro-5-Methylphenol in One-Component Solvents," *Rocz. Chem.*, **49**, 1879 (1975).
- Cocharan, W. G., "The Flow Due to a Rotating Disk," *Proc. Cambridge Phil. Soc.*, **30**, 365 (1934).
- Domanska, U., "Solid-Liquid Phase Relations of Some Normal Long-Chain Fatty Acids in Selected Organic One- and Two-Component Solvents," *Ind. Eng. Chem. Res.*, **26**, 1153 (1987).
- Dukler, A. E., "Dynamics of Vertical Falling Film Systems," *Chem. Eng. Prog.*, **55**, 62 (1959).
- Dukler, A. E., "The Role of Waves in Two Phase Flow: Some New Understandings," *Chem. Eng. Educ.*, **11**, 108 (1977).
- Dukler, A. E., and O. P. Bergelin, "Characteristics of Flow in Falling Liquid Films," *Chem. Eng. Prog.*, **48**, 557 (1952).
- Gallot-LaVallee, T., M. LaLande, and G. Corrieu, "An Optical Method to Study the Kinetics of Cleaning Milk Deposits by Sodium Hydroxide," *J. Food Eng.*, **5**, 131 (1982).
- Gregory, D. P., and A. C. Riddiford, "Transport to the Surface of a Rotating Disc," *J. Chem. Soc.*, 3756 (1956).
- Harris, J. C., R. M. Anderson, and J. J. Satanek, "Removal of Fatty Soil from Glass by Surfactants and Surfactant-Builder Compositions," *J. Amer. Oil Chem. Soc.*, **38**, 123 (1961).
- Harris, J. C., and J. J. Satanek, "Radiotagged Soils. Removal from Several Substrates and Adsorption Site Character," *J. Amer. Oil Chem. Soc.*, **38**, 244 (1961a).
- Harris, J. C., and J. J. Satanek, "Removal of Radio-Tagged Protein and Stearic Acid Soil from Glass," *J. Amer. Oil Chem. Soc.*, **38**, 169 (1961b).
- Hill, C. G., *An Introduction to Chemical Engineering Kinetics and Reactor Design*, Wiley, New York (1977).
- Iribarne, A., A. D. Gosman, and D. B. Spalding, "A Theoretical and Experimental Investigation of Diffusion-Controlled Electrolytic Mass Transfer Between a Falling Liquid Film and a Wall," *Int. J. Heat Mass Transfer*, **10**, 1661 (1967).
- Jennings, W. G., "Theory and Practice of Hard Surface Cleaning," *Adv. Food Res.*, **14**, 325 (1965).
- Kramers, H., and P. J. Kreyger, "Mass Transfer Between a Flat Surface and a Falling Liquid Film," *Chem. Eng. Sci.*, **6**, 42 (1956).
- LeClercq-Perlat, M. N., and M. LaLande, "A Review on the Modeling of the Removal of Porous Contaminants Deposited on Heat Transfer Surfaces," *Int. Chem. Eng.*, **31**, 74 (1991).
- Levenspiel, O., *Chemical Reaction Engineering*, 2nd ed., Wiley, New York, p. 27 (1972).
- Levich, V. G., *Physicochemical Hydrodynamics*, Prentice-Hall, Englewood Cliffs, NJ (1962).
- Mohr, C. M. J., and J. Newman, "Mass Transfer to an Eccentric Rotating Disk Electrode," *J. Electrochem. Soc.*, **122**, 928 (1975).
- Mohr, C. M. J., and J. Newman, "Mass Transfer to a Rotating Disk in Transition Flow," *J. Electrochem. Soc.*, **123**, 1687 (1976).
- Newman, J., *Electrochemical Systems*, Prentice-Hall, Englewood Cliffs, NJ (1973).
- Oliver, D. R., and T. E. Atherinos, "Mass Transfer to Liquid Films on an Inclined Plane," *Chem. Eng. Sci.*, **23**, 525 (1968).
- Perka, A. T., "A Mass-Transfer Model to Predict Reflux Cleaning Rates in Process Vessels," MS Thesis, North Carolina State Univ., Raleigh (1991).
- Perka, A. T., C. S. Grant, and M. R. Overcash, "Waste Minimization in Batch Vessel Cleaning," *Chem. Eng. Commun.*, **119**, 167 (1993).
- Plett, E. A., "Cleaning of Fouled Surfaces," *Fouling and Cleaning in Food Processing*, Univ. of Wisconsin, Madison, p. 288 (1985).
- Reid, R. C., J. M. Prausnitz, and T. K. Sherwood, *The Properties of Gases and Liquids*, McGraw-Hill, New York (1977).
- Schlichting, H., *Boundary Layer Theory*, McGraw-Hill, New York (1968).
- Smyrl, W. H., and J. Newman, "Limiting Current on a Rotating Disk with Radial Diffusion," *J. Electrochem. Soc.*, **118**, 1079 (1971).
- White, R., C. M. J. Mohr, and J. Newman, "The Fluid Motion Due to a Rotating Disk," *J. Electrochem. Soc.*, **123**, 383 (1976).
- Whitaker, S., *Fundamental Principles of Heat Transfer*, Krieger, FL (1977).
- Wragg, A. A., P. Serafimidis, and A. Einarsson, "Mass Transfer between a Falling Liquid Film and a Plane Vertical Surface," *Int. J. Heat Mass Transfer*, **11**, 1287 (1968).

Manuscript received Oct. 11, 1994, and revision received May 5, 1995.